Disentangling Variability in YSOs: Light Echoes, Diamond Stars, Ice and Accretion Diagnostics

Bringfried Stecklum & Verena Wolf (TLS Tautenburg)

Spitzer IRAC image of Cepheus A HW2

Light Echoes – From (NEO)WISE to Roman

YSO light echo (LE) basics

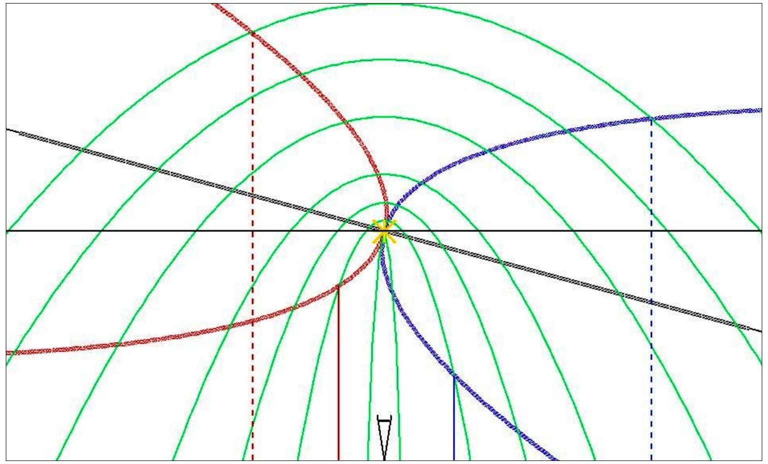

Single-scattering light echo (LE) geometry in a YSO

Photons emitted simultaneously propagate along **parabolic equal-time surfaces**.

Scattering at **cavity** **walls** produces asymmetric projected extents of the LE. Symmetry is recovered only for an inclination of 90° (edge-on disk).

Cep A HW2

M_{*}~10 $M_{\odot}$, L_{*}~2x10^4 $L_{\odot}$, d=700 pc, periodic 6.7 GHz masers (Durjasz+ 2022)

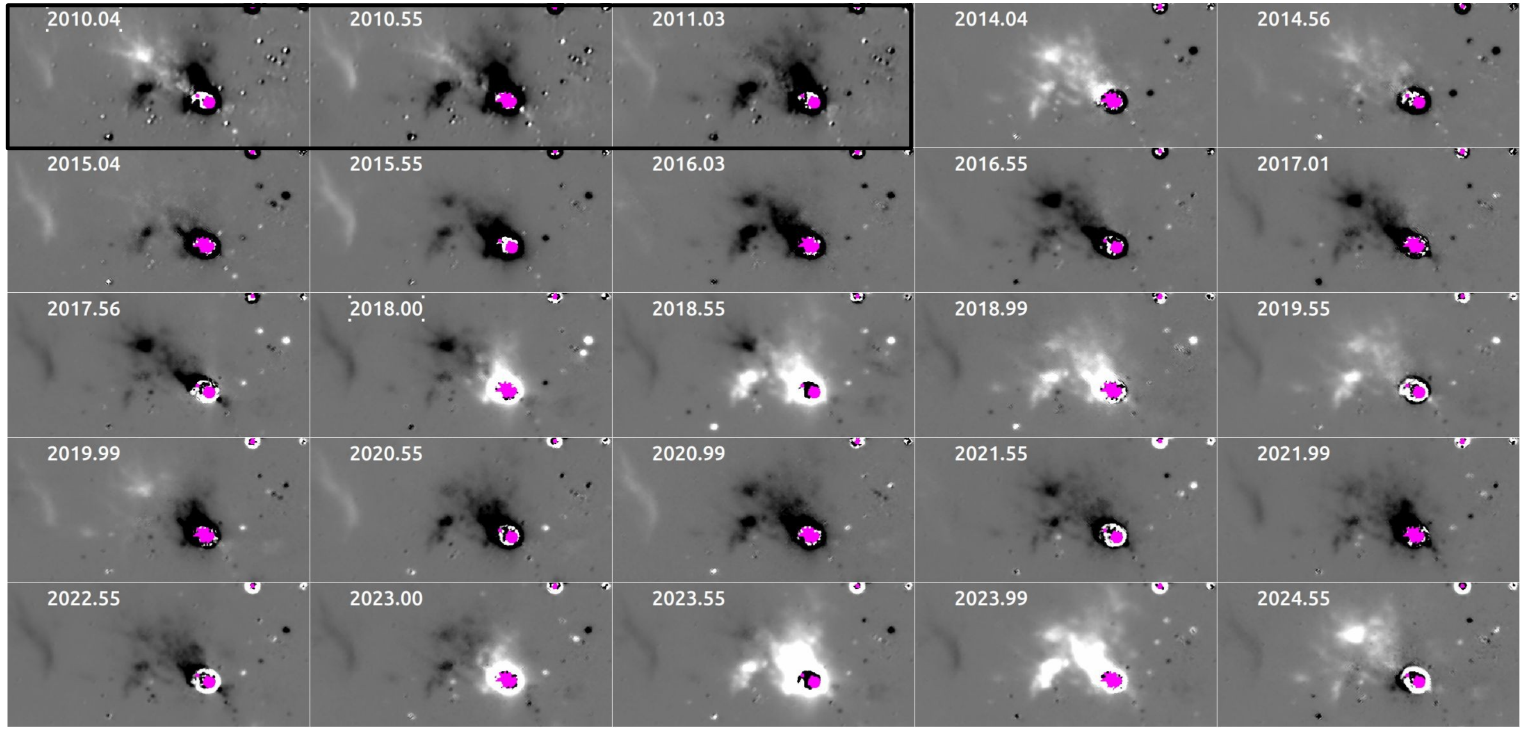

(NEO)WISE W1 difference frames (mean-subtracted, Magenta = saturated pixels)

LE shows periodic brightening/dimming (rectangle - WISE data).

Pixel-wise sinusoidal fits → period, amplitude & phase (Stecklum & Wolf 2025).

📌 Scattered light variability is an ubiquitous phenomenon, in particular for dust-enshrouded YSOs at substantial inclinations.

Light Echoes – From (NEO)WISE to Roman

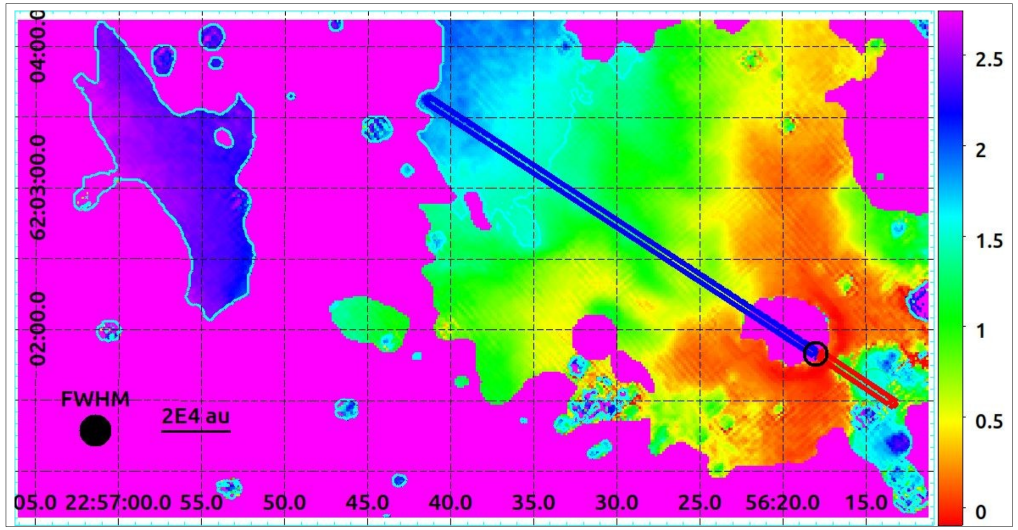

Phase map: time delay relative to Cep A HW2 (black circle)

Magenta: below noise threshold or saturated (near source)

Blueshifted outflow apparently more extended than **redshifted** lobe

Phase gradients along NE–SW axis imply disk inclination: 51° ± 11°

Near-source phase pattern resembles X-shaped outflow cavity walls

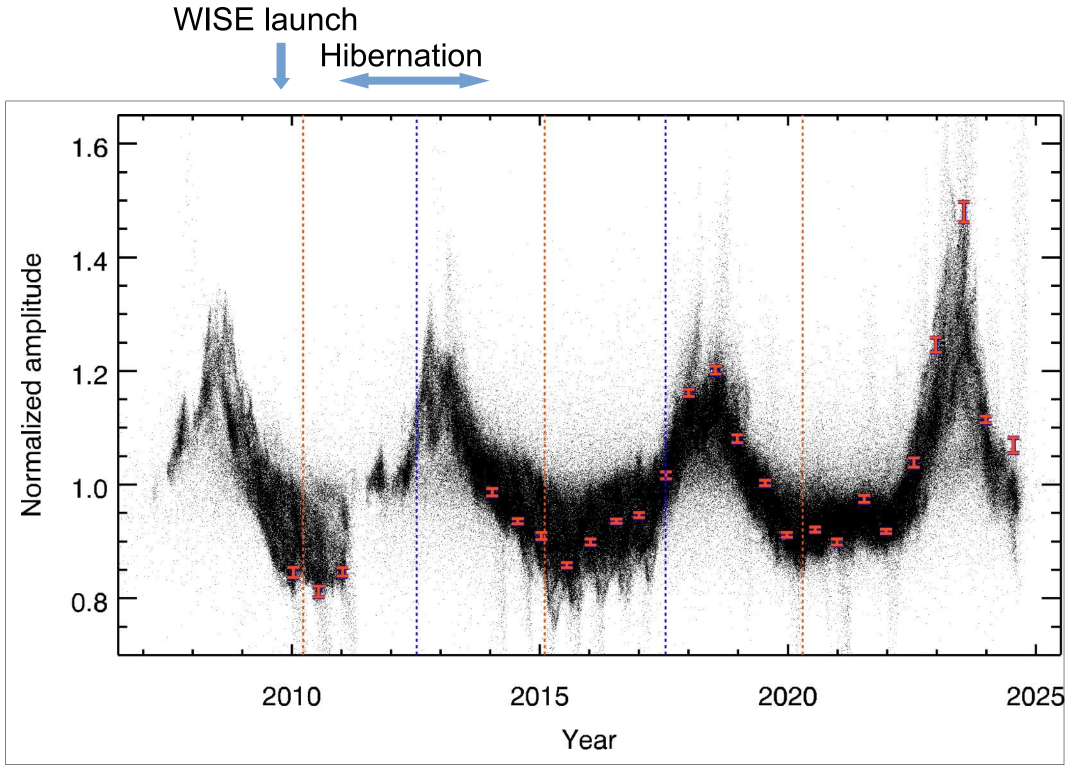

W1 light curve (reconstructed from phase shifts)

Full reconstruction spans four peaks, PSF-wing photometry (red) covers last two peaks only

Vertical lines: maser peak epochs (redshifted – red, blueshifted - blue) → anti-cyclic variability (Durjasz+ 2022)

Light Echoes – From (NEO)WISE to Roman

IRAS20126+4104

M_*~12 $M_\odot$, L_*~10^4 $L_\odot$, d=1.64 kpc

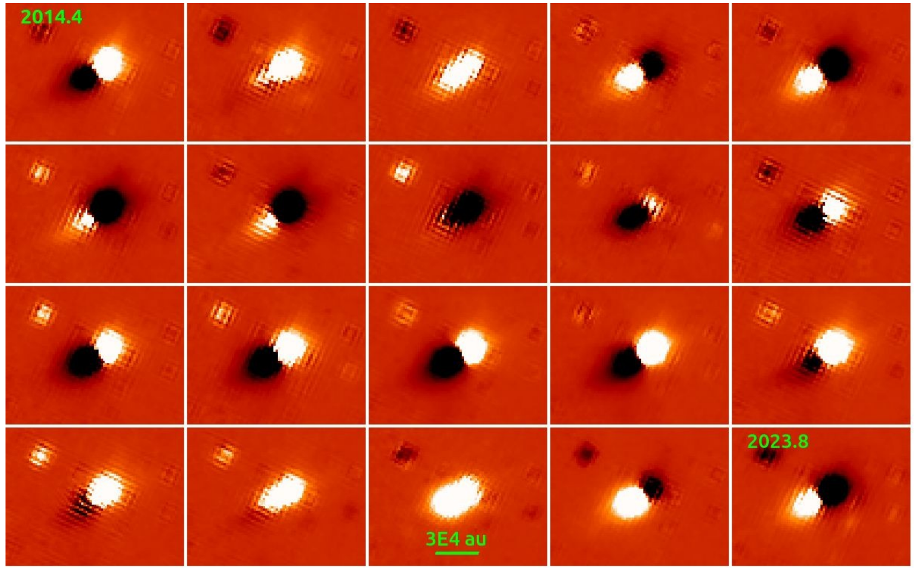

NEOWISE W1 difference frames (mean-subtracted) reveal anti-cyclic variability of the outflow lobes (cf. Cesaroni 2026).

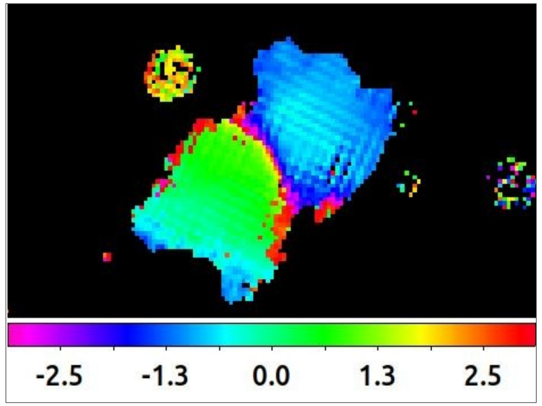

Our W1 phase map [rad] exhibits a dichotomy between the blue- and red-shifted lobes.

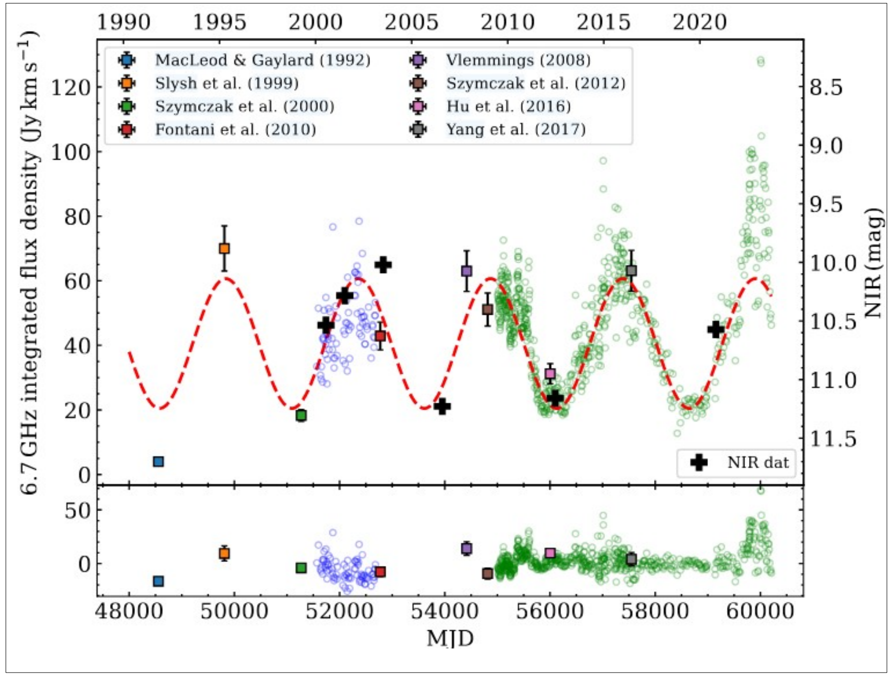

Integrated 6.7 GHz CH_3OH maser flux vs. time. The seven year period is obvious (Szymczak+ 2024).

Szymczak+ (2024) propose periodic eclipses of the central star by a wobbling inner disk induced by a nearby low-mass companion. This modulates both scattered light in the outflow lobes and maser pumping.

Cesaroni (2026) rejects this model because a precessing axisymmetric disk illuminates both lobes equally. This ignores scattering-geometry effects. Instead, he proposes a bloated star with a giant dark spot.

📌 Phase offsets between the outflow lobes point to a warp/tilt of the inner disk.

Modeling LEs

Mol3D radiative transfer code (Ober+ 2015)

Extended with photon time-tagging → time-dependent monochromatic scattering

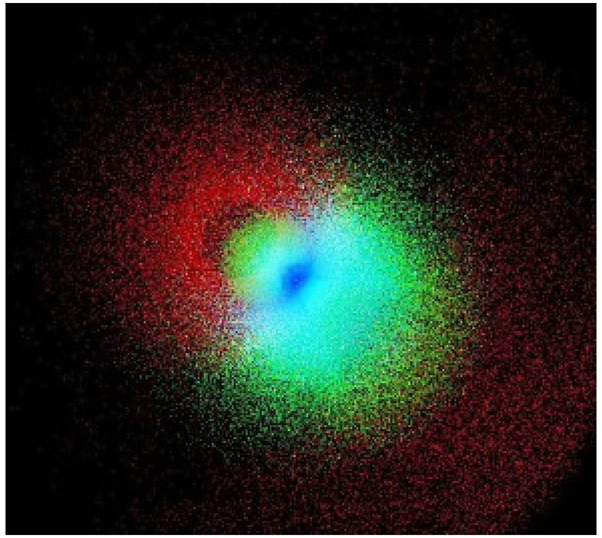

Light echo simulation (Class I YSO, i = 45°)

On-off outburst modeled with time-tagging extension
RGB image: synthetic snapshots at three observing times
(Wolf, in prep.)

Synthetic Ks-band difference images of L1527 IRS (Cook+ 2019)

Warped inner disk model (grey) with observed NIR contours at different azimuthal viewing angles (top left → bottom left): 0° to 180°
Strong scattering at cavity walls→ consistent with our W1 phase map (bottom right)

JWST's view on the object

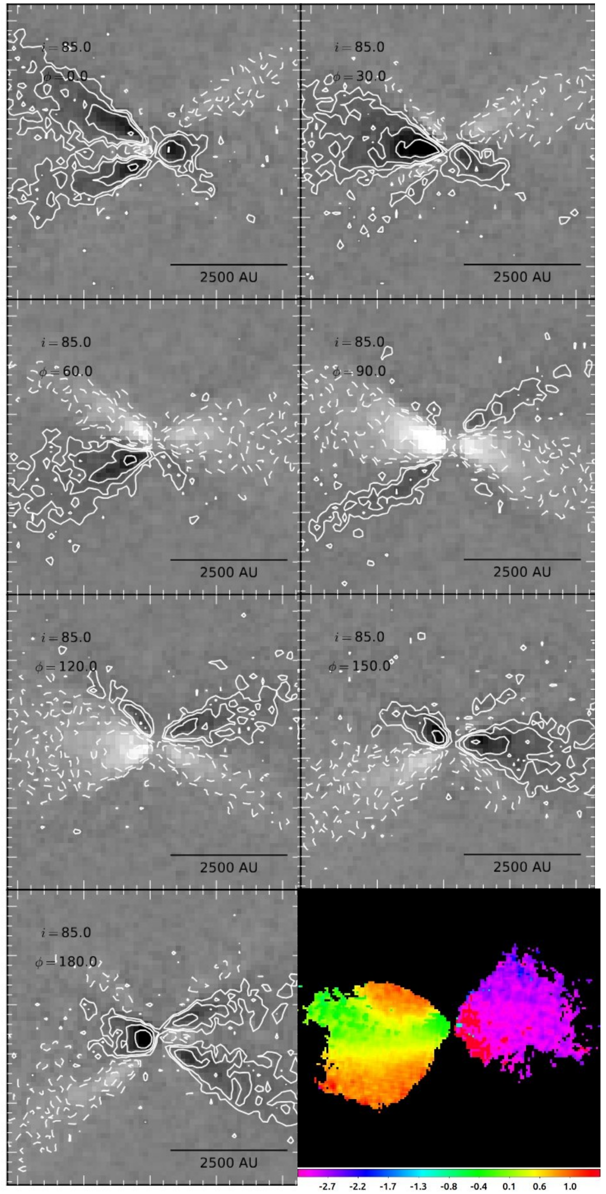

📌 LEs encode source variability, dust distribution, and viewing geometry, which can be recovered through Monte Carlo scattering models.

Diamond Stars – The Smoking Gun of Past Accretion Bursts?

Goodrich (1987) noted that all five FUors known at the time are associated with ring-shaped nebulae. For V1057 Cyg, Duncan+ (1981) suggested this could be illuminated material from a past outburst.
Are these structures expanding "smoke rings" of episodic accretion events?

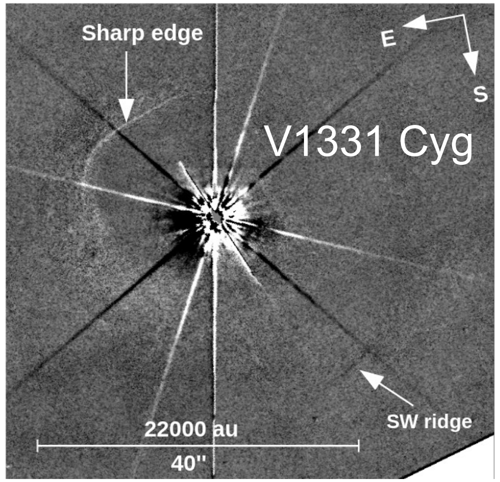

HST F606W, 2009 - 2000 difference image, outer arc expansion ~15 km/s (Choudhary & Stecklum 2016), consistent with CO ring (McMuldroch+ 1993)

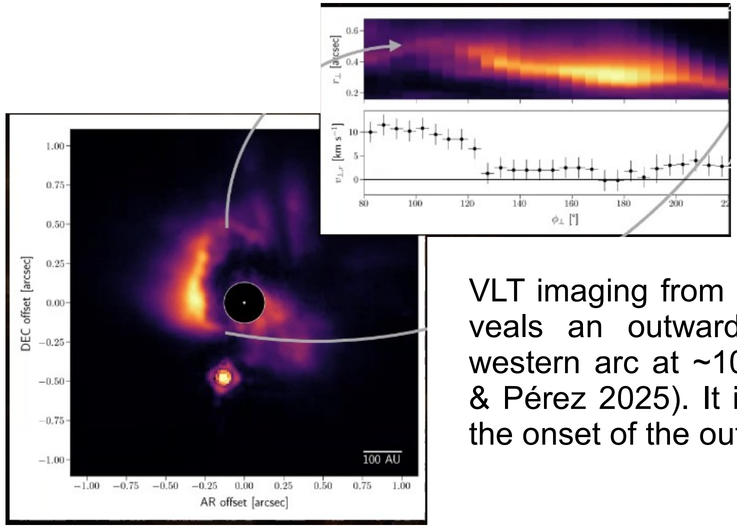

VLT imaging from 2017 to 2024 reveals an outward motion of the western arc at ~10 km/s (Calderon & Pérez 2025). It is consistent with the onset of the outburst in 1937.

JHKs image of Yun's+ (2007) "DiamondStar"

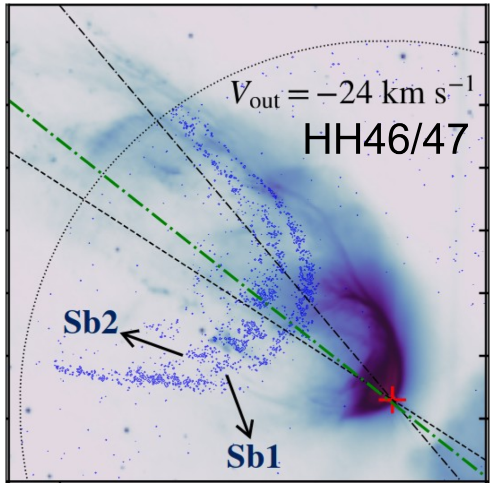

ALMA ^{12}CO observations show shell structures in the outflow lobes (Zangh+ 2026).

The ring-like appearance may arise at intermediate inclinations due to strong forward scattering and weak back-scattering and/or shadowing of the counter ring.

📌 Confirmation of ring expansion with Roman would enable back-dating of past accretion bursts and provide key constraints on the frequency of epi-sodic accretion.

Accretion Bursts and Water Ice

Example: S255IR-NIRS3 aka S255-IRS1

Accretion bursts sublimate ice and shift snowlines (e.g. Hsieh+ 2019), potentially weakening the 3.08 μm water-ice absorption feature.

Pre-burst optical depths from MIR spectra or the Δ(W1–I1) color excess (Meingast 2025) can be compared with post-burst SPHEREx measurements.

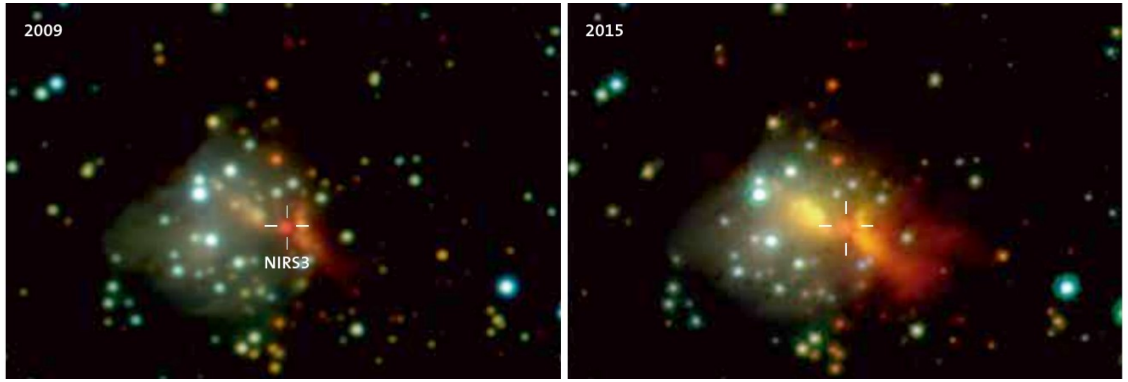

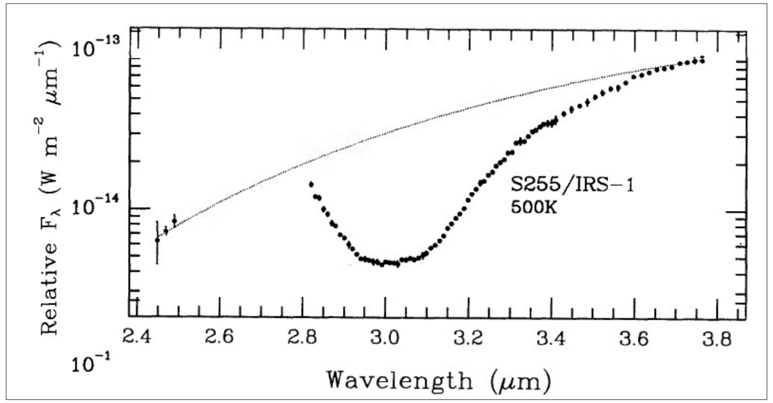

Water ice feature in S255-IRS1 (Smith+ 1989), epoch 1985, τ = 1.48

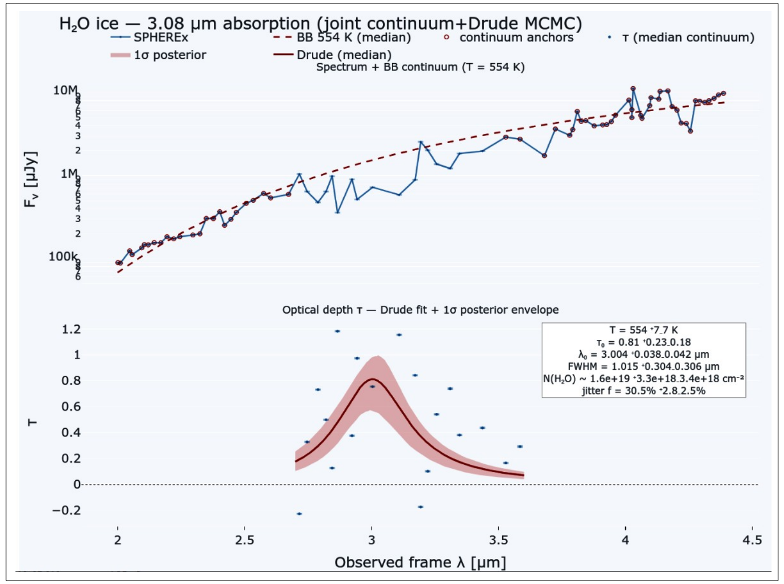

SPHEREx, epoch 2026, $\tau = 0.81^{+}0.23\ .0.18$

Preliminary result

📌 Envelope-dominated absorption may dilute burst-induced changes in the 3.08 μm ice feature. Nevertheless, embedded sources are predicted to exhibit the strongest ice depletion during bursts (Guadarrama+ 2024). Detectability is expected to depend on viewing geometry as well.

Accretion Diagnostics

Accretion rate - the quantitative measure of protostellar growth

T Tauri approach – use UV excess

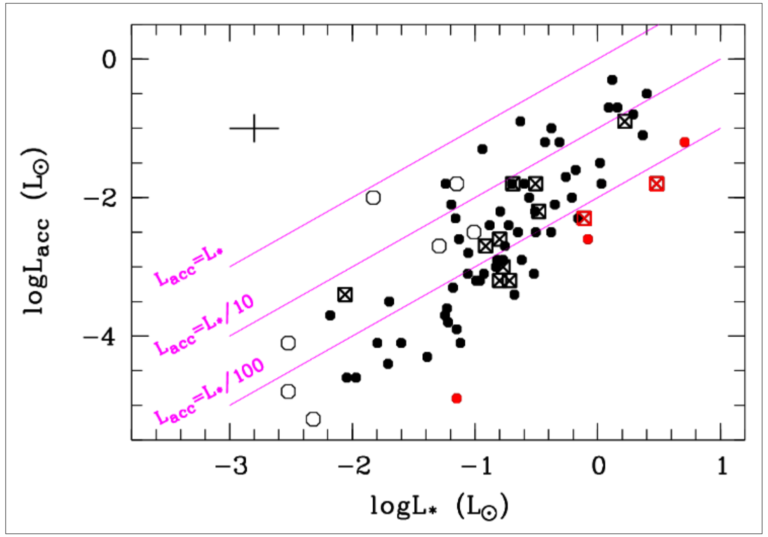

Accretion luminosity vs. stellar luminosity (Alcalá+ 2017). Folding in M_* and R_* yields accretion rates.

Despite extending to MIR HI lines (Testi+ 2025, Reyes-Reyes+ 2026) it is not applicable for

- Deeply embedded objects
- Very high accretion rates, but see Carvalho+ (2024)
- Absence of magnetospheric accretion
- Presence of winds and compact HII regions

MYSOs* - Bolometric luminosity changes

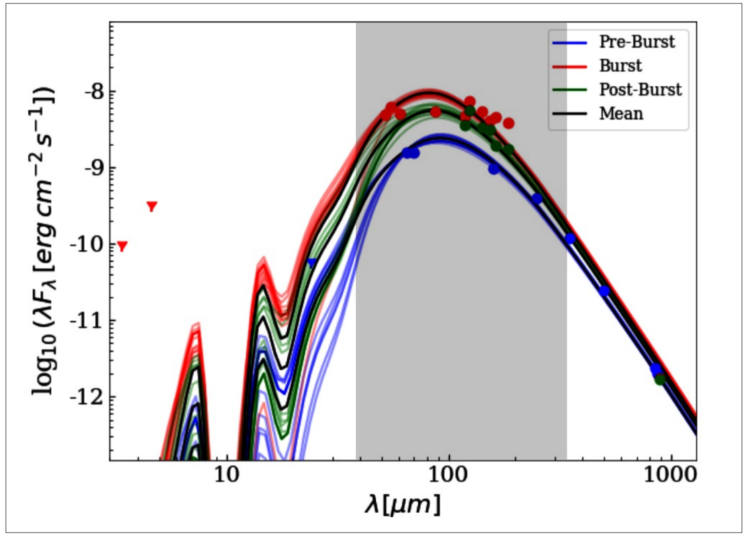

Pre-burst, **burst**, and **post-burst** SEDs of the MYSO G358-MM1 (Stecklum+ 2021). Triangles mark detection limits. Shaded range is inaccessible until PRIMA becomes reality.

- Requires well sampled SED
- Use radiative transfer modeling to account for anisotropy
- ZAMS radii yield lower limit

* Upper limit from redshifted molecular absorption lines (e.g., Beltran+ 2022)

Bridging the FIR gap

- **MIMIZUKU**@TAO, covers 2-38 μm (Kamizuka+ 2022)
- **CCAT-p,** covers 350-1300 μm

Supplement the SED

- **SPHEREx**: 0.75-5 μm, establishing SED, monitoring and discriminating extinction vs. luminosity changes.
- **NEOSurveyor**: 4.5 μm, 8 μm, monitoring, overlap with Galactic center/anticenter

📌 How strongly does the FIR gap degrade radiative-transfer constraints from SED modeling? Can variability compensate for the missing information?

Summary

Scattered light variability is an ubiquitous phenomenon, in particular for YSOs at substantial inclinations. Phase offsets between the outflow lobes point to a warp/tilt of the inner disk. LEs encode source variability, dust distribution, and viewing geometry, which can be recovered through Monte Carlo scattering models.

Confirmation of ring expansion with Roman would enable back-dating of past accretion bursts and provide key constraints on the frequency of episodic accretion.

Envelope-dominated absorption may dilute burst-induced changes in the 3.08 μm ice feature. Nevertheless, embedded sources are predicted to exhibit the strongest ice depletion during bursts (Guadarrama+ 2024). Detectability is expected to depend on viewing geometry as well.

How strongly does the FIR gap degrade radiative-transfer constraints from SED modeling? Can variability compensate for the missing information?

📌 While JWST is a superb facility, long-term monitoring and large-scale surveys require a complementary network of existing and upcoming observatories. Roman, SPHEREx, NEOSurveyor, and CCAT-prime will provide a multi-wavelength view of variability from the near-infrared to the submillimeter. This will reveal how accretion-driven changes across disks, envelopes, and outflows shape star and planet formation.